Thermodynamics of Deep Supercritical Geothermal Systems

IOP Conf. Series: Earth and Environmental Science **249** (2019) 012019 doi:10.1088/1755-1315/249/1/012019

Thermodynamics of Deep Supercritical Geothermal Systems

M C Suárez-Arriaga

Patzimba 438, Morelia, Mich., 58090 México

e-mail: mcsa50@gmail.com

Abstract. The study of water is very important in science and for many industrial applications, such as steam turbines, high pressure devices and supercritical cycles. In aquifers, hydrocarbon reservoirs, geothermal systems and atmosphere-ocean interactions, water is one of the most important fluids in action. Specifically, geothermal reservoirs contain water in a wide thermodynamic range. The temperature gradient between the core and the surface of the Earth results from a continuous flow of natural heat, embracing all kind of thermal energy resources that can be classified in terms of their profoundness, going from shallow depths (10^2 m), to medium depths (10^3 m), and to even deeper depths (10^4 m), reaching the immense temperatures of molten rocks. Warm aquifers below oil reservoirs, hot dry rock, submarine reservoirs, and engineered geothermal reservoirs are examples of profound geothermal systems. The fluids in very deep reservoirs can be at supercritical thermodynamic conditions, at more than 400°C and pressures larger than 220 bar, having higher fluid density, more volumetric enthalpy and heat available. They could provide twenty times as much power, per unit fluid volume, as the normal geothermal fluids used today. During the span of human life, deep geothermal energy represents practically an infinite potential. The aim of this paper is to provide a computational description of water thermodynamics at supercritical conditions showing the power it represents. The water properties are defined in terms of the Helmholtz potential or free energy, and are calculated for single phase, liquid, vapor and supercritical, as functions of density or pressure, and temperature. These properties are internal energy, enthalpy, entropy, specific isochoric heat, specific isobaric heat, compressibility, bulk modulus, Joule coefficient, speed of sound, thermal expansivity and thermal diffusivity.

1. Introduction

Humanity is consuming about 97 million barrels of oil/day (Mbd). Every year consumption grows by 1.5 Mbd (figure 1, https://www.iea.org/oilmarketreport/omrpublic/). On the other hand, there are about 1015 million automobiles circulating around the world, 35 million new cars are added each year. In many countries, at least 50% of oil demand is for transportation. In OECD countries the transport sector is responsible for almost 60% of oil consumption (http://www.iea.org/) and there is an overwhelming increase in the need for automotive fuel. Auto ownership is growing in India and in China; it is estimated that both countries could have 1.1 billion cars on the road by 2050. On the other hand, OPEC's oil spare capacity was 10 Mbd in 1995. Today this capacity is less than 2 Mbd; the world moved from a supply-led market to a demand-led one. In January 2018 the price of a barrel of Brent oil was $48 USD (figure 2, https://www.iea.org/oilmarketreport/omrpublic/). In May 2011 the same barrel costed $121 USD. In November 2010 its price was $88 USD and in July 2008 reached $145 USD the same barrel (http://www.oil-price.net/). There is no longer a safety margin to ensure price stability in the face of demand spikes and supply interruptions.

This year oil prices could go as high as $70 USD because several forces are putting pressure on oil value (growing worldwide global demand especially in China and India). The basic equation is: Limited Oil Supply + Increasing Demand = High Oil Prices.

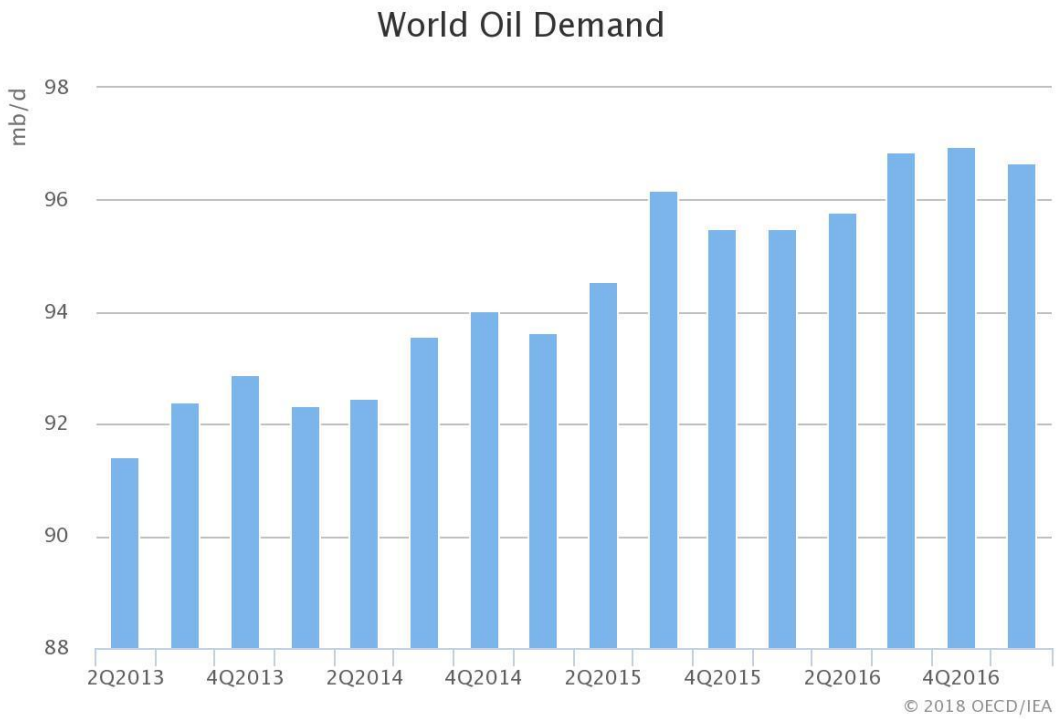

Figure 1. Worldwide oil consumption (Mbd) between 2013 and 2016.

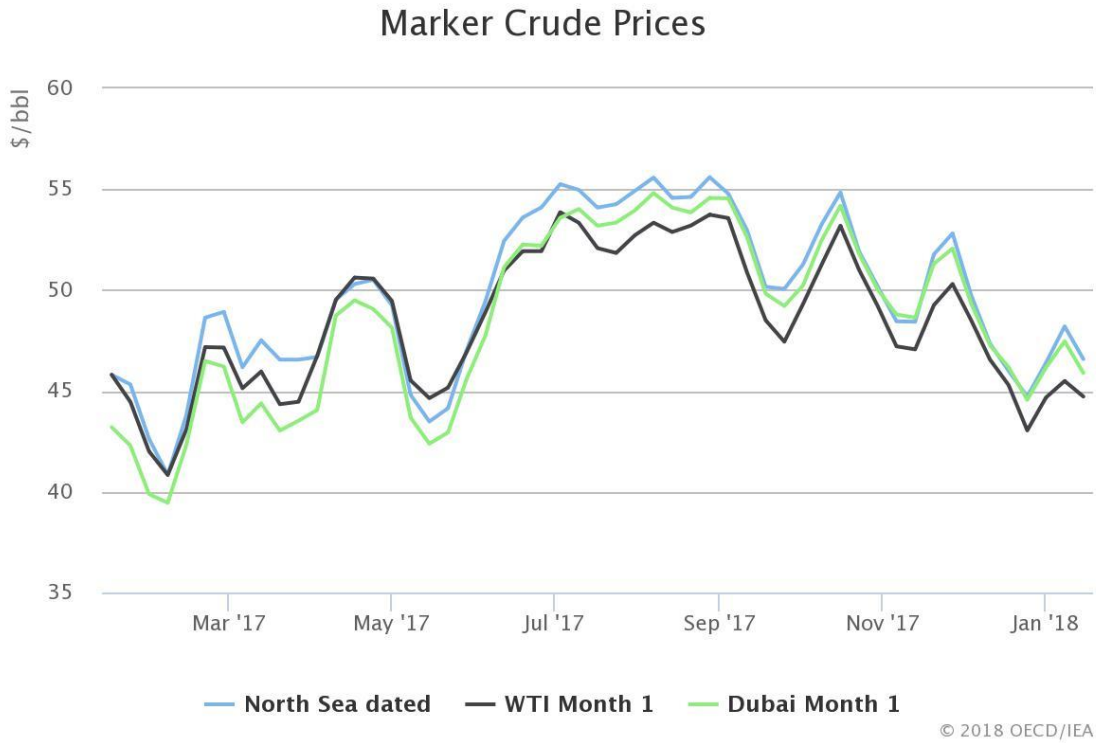

Figure 2. Oil prices (USD/barrel) between 2017 and 2018.

Soon or in a near future, the world could have limited petroleum supply, increasing demand with higher oil cost and increasing pollution with environmental impact. There is an urgent need to gradually replace hydrocarbons with other, diversified, and clean primary sources of energy. Deep geothermal energy is one of the main sources able to gradually replace hydrocarbons and nuclear. The intention of this paper is to provide a basic description of the properties and behaviour of geothermal water at supercritical conditions in deep reservoirs. These conditions correspond to an enormous energy source that has never been used on Earth.

2. Water thermodynamics and brief description of the Critical Point of water

Water in geothermal reservoirs covers a wide thermodynamic range, because the temperature gradient between the core and the surface of the Earth is producing a continuous flow of natural heat, going from shallow depths (10^2 m), to medium depths (10^3 m), and to even deeper depths (10^4 m), reaching the immense temperatures of molten rocks (T > 1000°C). The fluids in deep reservoirs are at supercritical thermodynamic conditions (T > 375°C, p > 220 bar), with higher fluid density and more heat available. These systems could provide twenty times as much power, as the normal geothermal fluids used today (T < 360°C, p < 100 bar).

2.1. Molecular structure of water

Water (H_2O) is a simple substance, but its properties show a complex behavior. Two hydrogen atoms and one oxygen atom make an angle of approximately 104.5 degrees, giving an extraordinary stability to this molecular structure: each hydrogen atom is in line between the oxygen atom on its own molecule and the oxygen atom of a different molecule (figure 3).

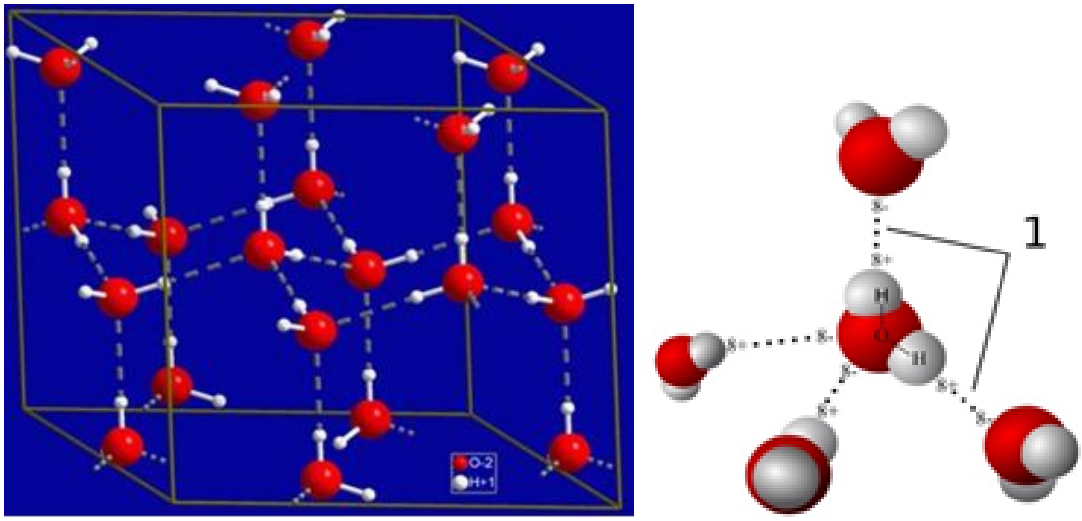

Figure 3. Molecules of water illustration, showing its structural bond (https://en.wikipedia.org/wiki/Hydrogen_bond, Public Domain).

Those hydrogen bonds have extra attractive energy, causing many of the unusual properties of water: 1) large heat of vaporization, 2) expansion upon freezing, 3) low thermal conductivity, 4) high specific heat, 5) very low liquid compressibility, 6) very high steam compressibility, 7) water is basic and acid at the same time (pKa/b = 15.74), 8) water is a universal solvent, 9) water reaches its maximum density at 4°C, and 10) below 4°C, water density declines.

The thermodynamic properties of ordinary water are functions of pressure and temperature in single phase systems. In two-phase systems p and T are related in the saturation line (K–Function), and another variable must be used; for example steam quality, liquid saturation or fluid enthalpy. As the critical point is approached the differences between thermodynamic properties of both phases vanish.

Once the critical point is reached, the latent heat of vaporization becomes zero and there is no more separation between both phases. In other words, the phase boundary between liquid and vapor disappears. We can also say that the distinction between vapor and liquid ends at the critical point.

2.1.1. Mathematical formulation of water properties. The International Association for the Properties of Water and Steam [1] published in 1995, a worldwide accepted mathematical formulation, which reproduces with maximum accuracy millions of experimental data obtained since 1824 up to present time. Water properties are calculated for single phase, liquid or vapor, as function of density and temperature (ρ, T), and for two-phase water (liquid and steam) pressure p is a function of saturation temperature p (T_{sat}). All water properties are constructed in terms of the Helmholtz potential (figure 4) defined as $f_w(\rho, T) = e_w - T s_w$, where e_w is internal energy and s_w is water entropy.

$$f_w(\upsilon_w, T) = e_w - T s_w \;\Rightarrow\; d f_w = -p\, d\upsilon_w - s_w\, dT \;\Rightarrow\; p = -\frac{\partial f_w}{\partial \upsilon_w},\; s_w = -\frac{\partial f_w}{\partial T} \tag{1}$$

Where $\upsilon_w = \rho^{-1}$ is specific volume. The potential f_w becomes dimensionless (Φ) as follows:

$$\delta = \frac{\rho}{\rho_C},\; \tau = \frac{T_C}{T} \;\Rightarrow\; \frac{f_w(\rho, T)}{R\,T} = \Phi(\delta, \tau) = \Phi^{gas-ideal} + \Phi^{residual} = \Phi^0(\delta, \tau) + \Phi^r(\delta, \tau) \tag{2}$$

Where δ and τ are dimensionless density and inverse temperature respectively; the values of the critical constants are:

$$\rho_C = 322.0\ \frac{\text{kg}}{\text{m}^3},\; T_C = 647.096\ \text{K},\; P_C = 22.064\times10^6\ \text{Pa},\; \mu_C = 10^{-6}\ Pa\cdot s,\; R = 0.46151805\ \left[\frac{\text{kJ}}{\text{kg K}}\right]$$

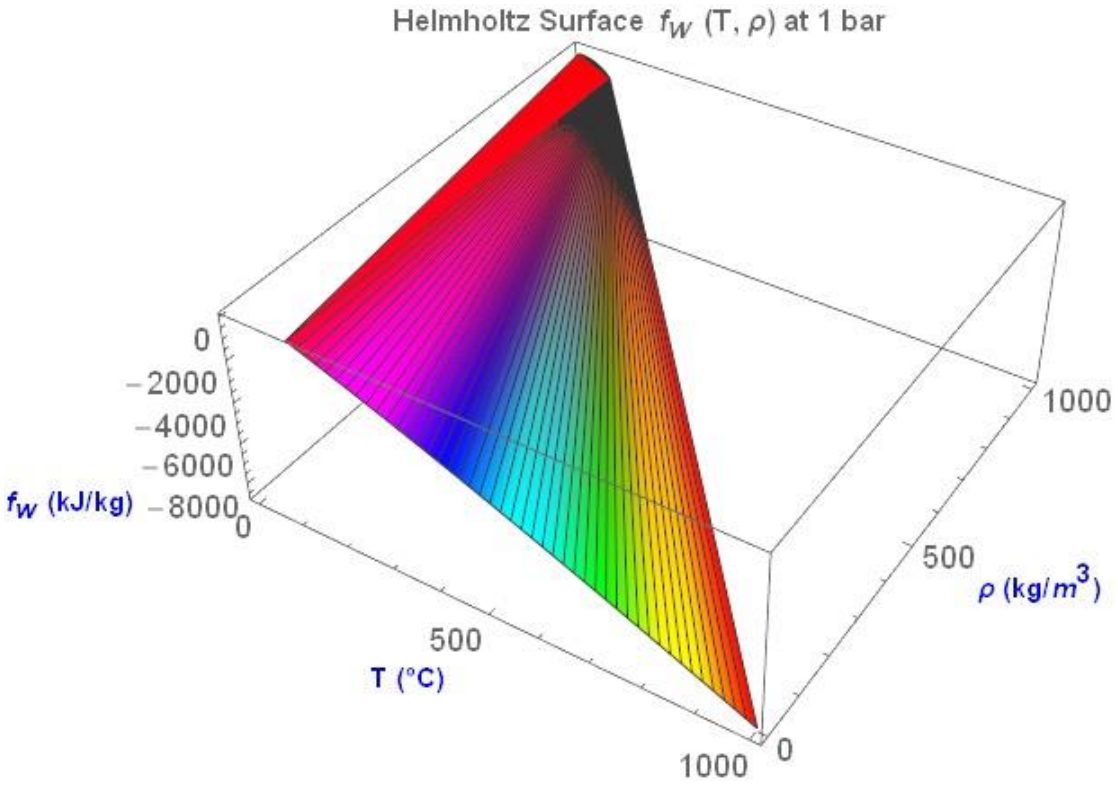

Figure 4. Helmholtz 3D surface for water showing its values at 1 bar and 0 ≤ T ≤ 1000 °C.

The mathematical form of the ideal gas part (Φ^0) and the residual part (Φ^r) of Φ was built by the *International Association for the Properties of Water and Steam* (http://www.iapws.org/):

$$\Phi_{gas}^{ideal} = \Phi^0(\delta,\tau) = Log(\delta) + n_{01} + n_{02}\,\tau + n_{03}\,Log(\tau) + \sum_{i=4}^{8} n_{0i}\,Log\left(1-e^{-\gamma_{0i}\tau}\right)$$
$$\Phi^r(\delta,\tau) = \sum_{i=1}^{7} n_i\,\delta^{d_i}\tau^{t_i} + \sum_{i=8}^{51} n_i\,\delta^{d_i}\tau^{t_i}e^{-\delta^{c_i}} + \sum_{i=52}^{54} n_i\,\delta^{d_i}\tau^{t_i}e^{-\alpha_i(\delta-\varepsilon_i)^2-\beta_i(\tau-\gamma_i)^2} + \sum_{i=55}^{56} n_i\,\Delta^{b_i}\delta\,\psi \quad (3)$$

Where the auxiliary functions are defined as follows:

$$\Delta(\delta) = \Theta^2 + B_i(\delta-1)^{2a_i};\ \Theta(\delta,\tau) = 1-\tau + A_i(\delta-1)^{\frac{1}{\beta_i}};\ \psi(\delta,\tau) = e^{-C_i(\delta-1)^2 - D_i(\tau-1)^2} \quad (4)$$

All numerical coefficients included in these formulae, are defined and detailed in the same reference [1]. The combination of both parts of the dimensionless potential Φ define a full Helmholtz surface given by equation (2). Other thermodynamic properties of water are obtained by partial differentiation over the Helmholtz potential or free energy surface:

$$p = \rho^2\left(\frac{\partial f_w}{\partial\rho}\right)_T,\ e = f_w - T\left(\frac{\partial f_w}{\partial T}\right)_\rho,\ h = f_w - T\left(\frac{\partial f_w}{\partial T}\right)_\rho + \rho\left(\frac{\partial f_w}{\partial\rho}\right)_T,\ s = -\left(\frac{\partial f_w}{\partial T}\right)_\rho$$
$$c_V = \left(\frac{\partial e}{\partial T}\right)_V,\ c_p = \left(\frac{\partial h}{\partial T}\right)_p,\ C_f = \frac{1}{\rho}\left(\frac{\partial\rho}{\partial p}\right)_T,\ J = \left(\frac{\partial T}{\partial p}\right)_h,\ v_s = \sqrt{\left(\frac{\partial p}{\partial\rho}\right)_s},\ \gamma_f = \frac{-1}{\rho}\left(\frac{\partial\rho}{\partial T}\right)_p \quad (5)$$

Where symbols h, c_V, c_p, C_f, J, v_s and γ_f are specific enthalpy, isochoric and isobaric heat, isothermal compressibility, Joule-Thomson coefficient, sound speed and isobaric thermal expansion respectively. Thermal diffusivity can also be computed as:, $\delta_f = k_T/\rho\,c_p$, where k_T is the thermal conductivity of the fluid. All the properties given in equation (5) are computed in terms of the dimensionless parts of the Helmholtz potential:

1). $p(\delta,\tau) = R\,\rho_C\,T_C\,\tau^{-1}\left(\delta + \delta^2\frac{\partial\Phi^r}{\partial\delta}\right)$, 2). $e(\delta,\tau) = R\,T\,\tau\left(\frac{\partial\Phi^0}{\partial\tau} + \frac{\partial\Phi^r}{\partial\tau}\right)$,

3). $h(\delta,\tau) = R\,T\left(1+\tau\left(\frac{\partial\Phi^0}{\partial\tau} + \frac{\partial\Phi^r}{\partial\tau}\right)\right)$, 4). $s(\delta,\tau) = R\left(\tau\left(\frac{\partial\Phi^0}{\partial\tau} + \frac{\partial\Phi^r}{\partial\tau}\right) - \Phi^0 - \Phi^r\right)$,

5). $c_V(\delta,\tau) = -R\,\tau^2\left(\frac{\partial^2\Phi^0}{\partial\tau^2} + \frac{\partial^2\Phi^r}{\partial\tau^2}\right)$, (6a)

6). $c_p(\delta,\tau) = R\left(-\tau^2\left(\frac{\partial^2\Phi^0}{\partial\tau^2} + \frac{\partial^2\Phi^r}{\partial\tau^2}\right) + \frac{1+\delta\frac{\partial\Phi^r}{\partial\delta} - \delta\,\tau\frac{\partial^2\Phi^r}{\partial\delta\,\partial\tau}}{1+2\,\delta\frac{\partial\Phi^r}{\partial\delta} + \delta^2\frac{\partial^2\Phi^r}{\partial\delta^2}}\right)$,

7). $K_f(\delta,\tau) = \frac{R\,\rho_C\,T_C}{\tau}\left(\delta + 2\delta^2\frac{\partial\Phi^r}{\partial\delta} + \delta^3\frac{\partial^2\Phi^r}{\partial\delta^2}\right)$, 8). $C_f(\delta,\tau) = \frac{1}{K_f(\delta,\tau)}$

$$9).\ v_S(\delta,\tau)=\sqrt{R\,T\times10^3\left(1+2\,\delta\frac{\partial\Phi^r}{\partial\delta}+\delta^2\frac{\partial^2\Phi^r}{\partial\delta^2}-\frac{\left(1+\delta\frac{\partial\Phi^r}{\partial\delta}-\delta\,\tau\frac{\partial^2\Phi^r}{\partial\delta\,\partial\tau}\right)^2}{\tau^2\left(\frac{\partial^2\Phi^0}{\partial\tau^2}+\frac{\partial^2\Phi^r}{\partial\tau^2}\right)}\right)} \tag{6b}$$

$$10).\ \gamma_f(\delta,\tau)=\frac{\tau^2}{T_C\,\delta}\left(\frac{\partial\delta}{\partial\tau}\right)_\Pi,\quad 11).\ \delta_f(\delta,\tau)=\frac{k_T}{\rho_C\,\delta\,c_p(\delta,\tau)}$$

Thermal conductivity of water, including a critical enhancement, is calculated separately [2]:

$$\theta=\frac{T}{T_C}=\tau^{-1},\ \lambda_2(\delta,\tau)=\frac{\Lambda}{\tau}\frac{\delta\,c_p(\delta,\tau)\mu_c}{R\,\mu_{f0}}Z(y_0)\Rightarrow k_T(\theta,\delta)=\lambda_0(\theta)\,\lambda_1(\theta,\delta)+\lambda_2(\theta,\delta)$$
$$\lambda_0(\tau)=\sqrt{\tau^{-1}}\left(\sum_{i=0}^{4}L_i\,\tau^i\right)^{-1};\quad \lambda_1(\delta,\tau)=\mathrm{Exp}\left[\delta\sum_{i=0}^{4}(\tau-1)^i\times\sum_{j=0}^{5}L(i,j)(\delta-1)^j\right] \tag{7}$$

Dynamic viscosity is computed as follows [1]:

$$\mu_w(\delta,\theta)=\mu_0(\delta,\theta)\,\mu_1(\delta,\theta),\ \theta=\tau^{-1},\ \mu_0(\delta,\theta)=100\sqrt{\theta}\times\left(\sum_{i=0}^{3}\frac{H_i}{\theta^i}\right)^{-1}$$
$$\mu_1(\delta,\theta)=Exp\left[\delta\sum_{i=0}^{5}\left(\frac{1}{\theta}-1\right)^i\sum_{j=0}^{6}H_{ij}(\delta-1)^j\right] \tag{8}$$

2.2. Range of validity and definite limits of this formulation for water

The IAPWS R6-95 covers the five phases of water (solid, liquid, steam, two-phase and supercritical), in the entire stable fluid region for $p \in$ [0.1, 10,000] bar, and for $T \in$ [0, 1000]°C (1273 K), reproducing with high precision all the experimental data available at the time the release 2016 of the IAPWS-95 was prepared, including the critical point (374°C, 221 bar, 322 kg/m^3, 2085 kJ/kg). The interpolating equations of this formulation can be extrapolated for density and enthalpy beyond the already mentioned limits, giving reasonable accurate results for pressures up to 10^6 bar and temperatures up to 4727 °C (5000 K). All functions and derivatives are computed as functions of (δ, τ) in IAPWS-95. In geothermal fields, for practical reasons, it is more efficient to use the variables (p, T) because water density is not measured. A backward formulation entirely based on the IAPWS-95 was created [3] using a two-dimensional projection of the Newton-Raphson algorithm, which attains convergence in less than three ($n \leq 3$) iterations ($0 \leqslant$ error $\leqslant 10^{-9}$):

$$\boxed{\delta_{n+1}=\delta_n-\left(\frac{R\,\rho_C\,T_0}{P_C}\left(\delta_n+\delta_n^2\frac{\partial\Phi^r(\delta_n,\tau_0)}{\partial\delta}\right)-\frac{p_0}{P_C}\right)\frac{\partial\delta}{\partial\Pi}(\delta_n,\tau_0)}\ \Rightarrow\ \boxed{\rho(p_0,T_0)\simeq\rho_C\,\delta_{n+1}} \tag{9}$$

where: $\left(\frac{\partial\delta}{\partial\Pi}\right)^{-1}=\frac{K_f(\delta,\tau)}{P_C\,\delta}=\frac{R\,\rho_C\,T}{P_C}\left(1+2\,\delta\frac{\partial\Phi^r}{\partial\delta}+\delta^2\frac{\partial^2\Phi^r}{\partial\delta^2}\right),\quad \Pi=\frac{p}{P_C}$

Figure 5 shows the main regions mentioned in the above paragraph, including the ice zones and the critical point. The supercritical zone is above to the right of this point.

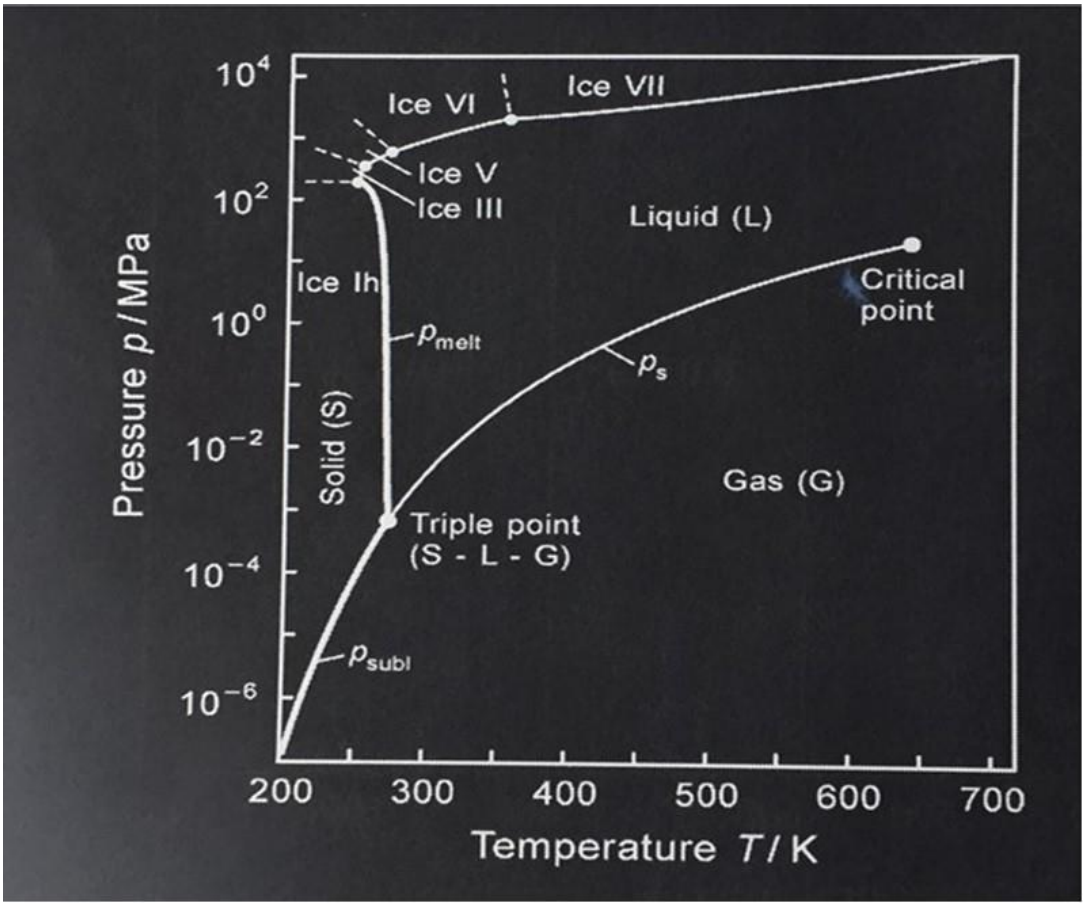

Figure 5. Thermodynamic regions of water projected in a (p, T) plane within the ranges indicated [1].

3. Thermodynamics of the Supercritical region of water

There are several ways to define the critical point of water. In a pure water temperature-specific volume diagram, the critical point is an inflection point with a zero slope. At this critical point the saturated-liquid and saturated-vapor states become equal in every respect. This point is a small region located between [373.5, 374.5] °C, showing discontinuities in density between [280, 380] kg/m^3 and in enthalpy between [2000, 2150] kJ/kg. In this zone any change in pressure or in temperature produces wide density and enthalpy changes. Isobaric specific heat, isothermal compressibility, thermal conductivity, and dynamic viscosity also exhibit large gradients when pressure changes in a neighborhood of the critical point (see figures 9-12). The basic properties of water at the critical point are defined by specific numerical values: the critical temperature is 374°C (T_C = 647.096 K), the critical pressure is 221 bar (P_C = 22.064 MPa), the critical density ρ_C is 322 kg/m^3, and the critical enthalpy h_C is 2100 kJ/kg [1]. At the critical point the densities of the two phases become identical. This collapse of both phases originates discontinuities which are present in all the thermodynamic properties. Above the critical temperature water can exist only as a supercritical fluid and no liquefaction can occur, no matter how high the pressure is raised. One important characteristic of supercritical water is that its solubility capacity increases with pressure in every isothermal curve.

Beyond the critical point (figures 5, 6) there is only one single phase which is called supercritical water defining a whole thermodynamic zone, the supercritical region (figure 6). During any isobaric process at a pressure greater than the critical pressure, or in isothermal processes at temperatures above the critical temperature, there will never be two phases present, because vapor and liquid merge into a single phase. Only changes in density will be observed when the temperature or the pressure

changes. Geothermal fluids are complex mixtures of water, and diverse amounts of salts and gases; obtaining precisely the diverse critical points of these mixtures is a complicated experimental problem not yet solved. But physical intuition indicates that their behavior would be similar or parallel to the behavior of ordinary water in the supercritical region.

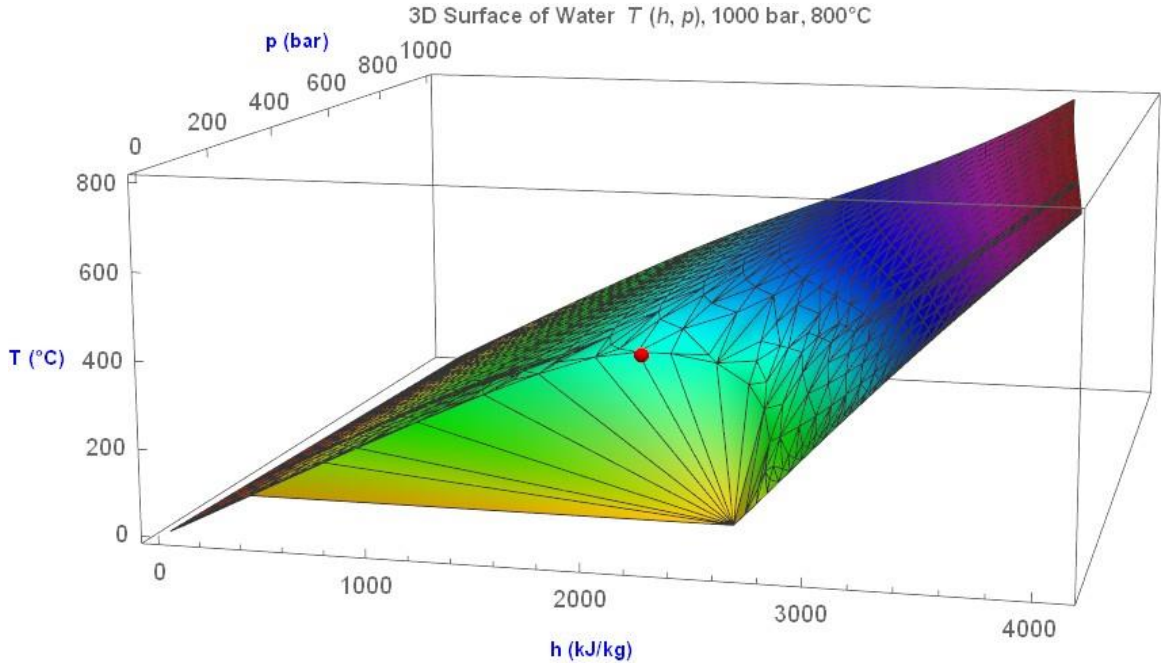

Figure 6. Temperature 3D surface as function of enthalpy and pressure in the range [0, 800] °C.

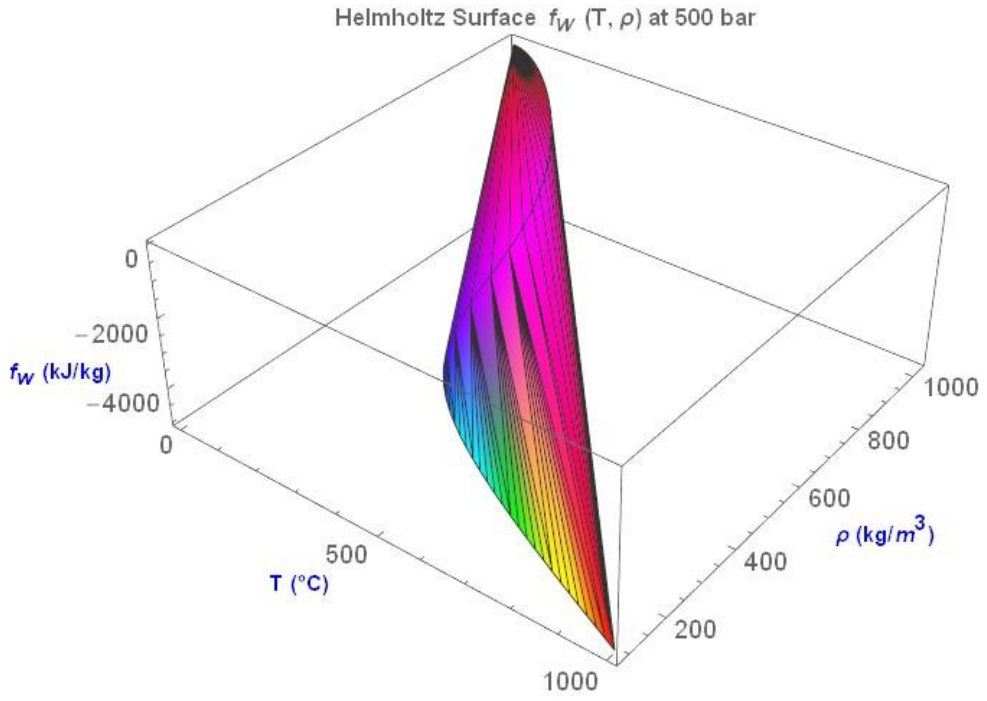

Figure 7. Corresponding 3D Helmholtz surface including the supercritical region of 500 bars.

Figures 6 and 7 cover the most common geothermal range for practical use and include a portion of the supercritical zone. The curved region below the critical point in the 3D surface of figure 6, corresponds to the two-phase zone of water. The liquid region is located to the left of this zone, the superheated steam region is above it, and the supercritical zone is up to the right. The red ball shows the approximate location of the critical point in the plane (*h, T*).

Any deep geothermal system reaching enough pressure and temperature can be at supercritical conditions. For example, submarine reservoirs, which are related to the existence of hydrothermal vents emerging in many places along the oceanic spreading centers between tectonic plates. In these sites, hydrothermal fluid at 350°C - 400°C exits the seafloor through natural chimneys at velocities of about 70 to 236 cm/s and mixes with seawater at 4°C at more than 2000 m depth. These systems have a total length of about 65,000 km in the oceanic crust and contain huge amounts of energy. They represent one of the primary modes of interaction between the solid earth and the ocean/atmosphere system [4]. The specific chemical characteristics of submarine hydrothermal deep systems indicate that water-oceanic rock interactions occur at supercritical temperature and pressure conditions.

3.1. Properties of supercritical water in graphic form

The following figures illustrate the most common thermodynamic properties of water as functions of temperature and pressure in the supercritical region of [374, 1000] °C and [220, 1000] bar. The figures include the region 300°C ≤ T ≤ 374°C as a starting zone. The data were obtained using the NIST/ASME Steam Properties software, version 2.21 [5], which is based on the same formulation [1].

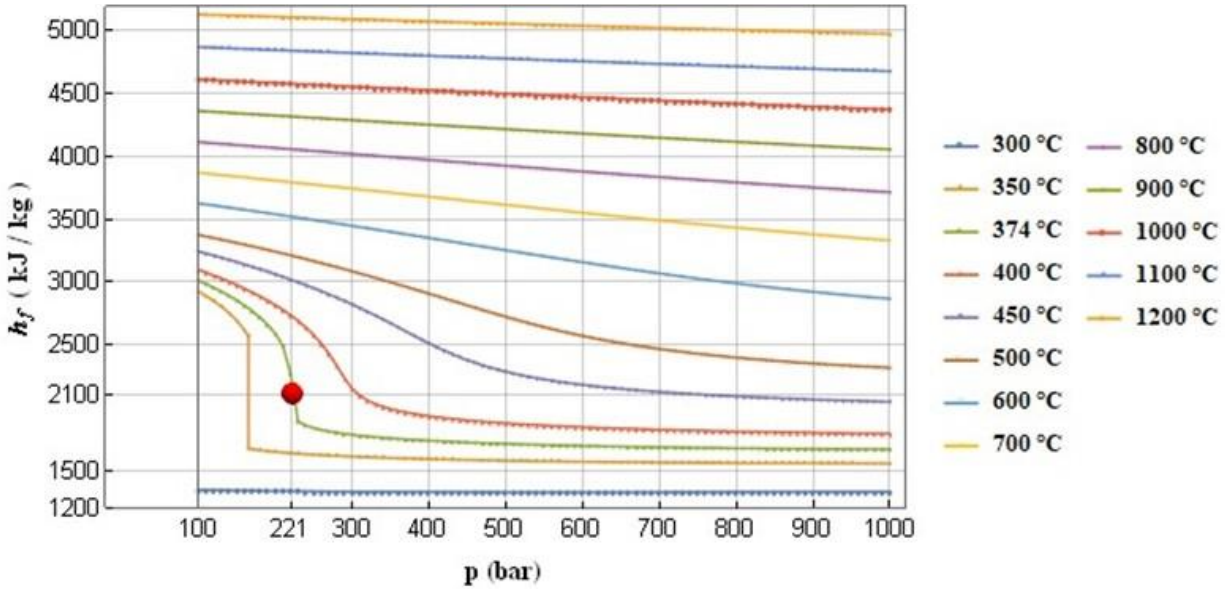

Figure 8. A portion of the supercritical zone projected into the plane (p, h_f) with different temperatures 300 ≤ T ≤ 1200°C, the red ball represents the critical point.

3.1.1. Density and enthalpy at supercritical conditions. The following graphics show different water properties as function of temperature for the shown pressures. The values of supercritical density diminishe when temperature increases, but they are larger than 120 kg/m^3 at 400°C at the starting pressure of 220 bar (Figure 9a). At higher pressures the supercritical density increases. This physical fact has a huge importance when computing the volumetric enthalpy of supercritical water. The specific water enthalpy increases with temperature and decrease when the supercritical pressure increases (figure 9b). The missing points in both figures at 220 bars, are real discontinuities near the critical point.

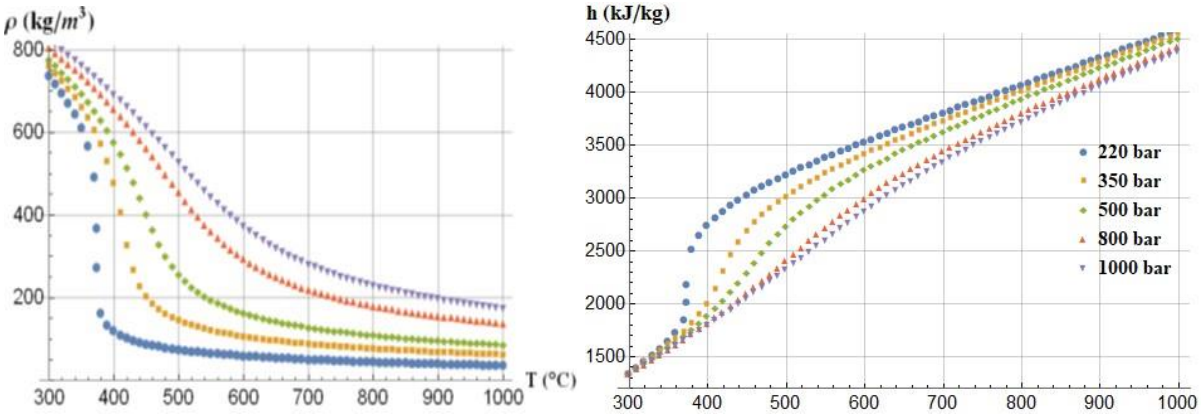

Figure 9. a) Density (left) and b) enthalpy (right) in the supercritical zone at different pressures.

3.1.2. Dynamic viscosity and thermal conductivity at supercritical conditions. Next figures show that the behaviour of both properties is similar in shape: they decrease before the temperatures between 400 and 700°C, at the shown respective pressures. After these points, they increase linearly or remain constant. Thermal conductivity clearly shows a region of discontinuity around the critical point.

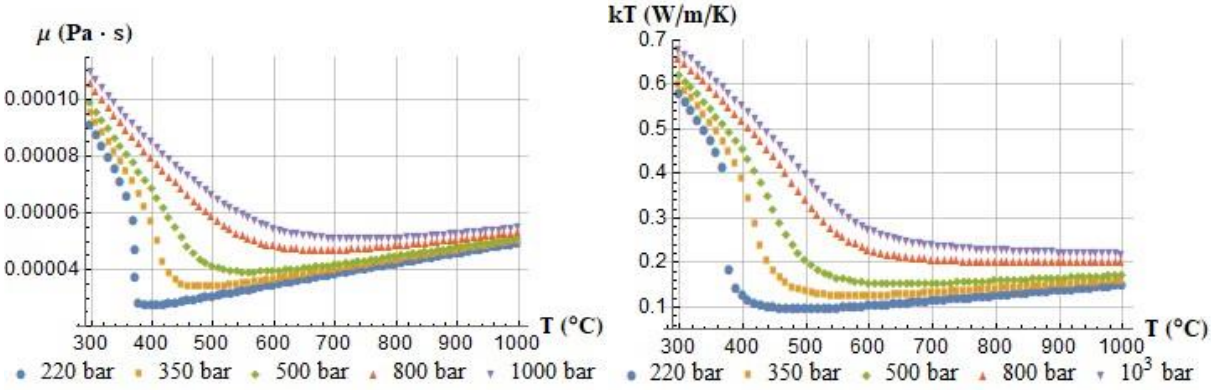

Figure 10. a) Dynamic viscosity (left) and b) thermal conductivity (right) in the supercritical zone.

3.1.3. Isobaric specific heat. Figure 11 shows that c_p increases beyond any realistic physical limit around 374°C. Extremely high values of c_p have no physical meaning and must be considered as divergent numerical outcomes in the partial differential equations (6) as explained in [3].

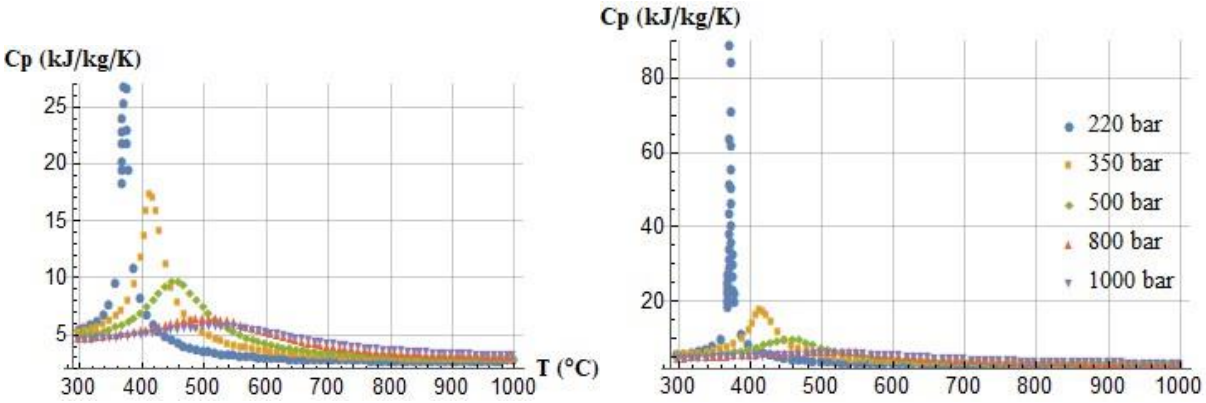

Figure 11. Discontinuity with sudden increment of the specific heat around the critical point.

3.1.4. Isothermal compressibility and bulk modulus. Both properties are the inverse of each other, but it is interesting to see the behaviour of each one of them separately. It is well known that water compressibility increases with temperature before the critical point at any pressure. In the supercritical zone it decreases after the critical point and remains almost constant when temperature increases (figure 12a), also showing discontinuities around the critical point. The bulk modulus decreases significantly when temperature rises and increases slightly with supercritical pressures (figure 12b). It is important to note that its value at 220 bar and 25°C is 2.1 GPa. At 220 bar and 400°C the bulk modulus of water equals 0.0104 GPa. This means that the bulk modulus in supercritical reservoirs is more than 200 times smaller than in cold aquifers. This coefficient is involved in several relationships among other poroelastic modules [6]. This numerical difference shows the determinant influence of temperature on rock thermoporoelastic behaviour. The main general trend is that rock deformation is larger in geothermal supercritical reservoirs than in normal cold or warm aquifers.

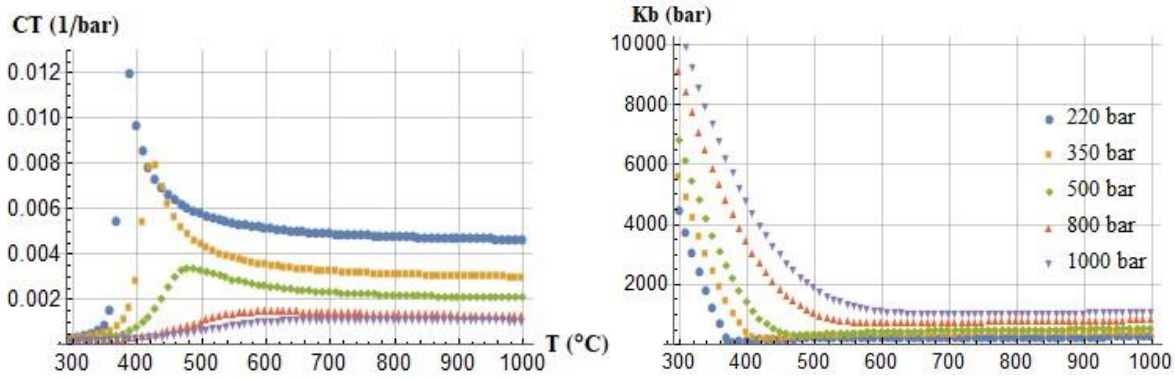

Figure 12. Isothermal compressibility (left) and bulk modulus (right) of supercritical water.

4. Volumetric enthalpy and exergy of supercritical systems

The change of specific enthalpy in a reservoir is the heat extracted during a process under constant pressure. This change includes both the change in internal energy and the work done, it is equal to the isobaric heat transfer δQ_p during the process:

$$\Delta h_w(p, s_w) = \Delta e_w + p\Delta \upsilon_w = \left(\delta Q_p - p\Delta \upsilon_w\right) + p\Delta \upsilon_w = \delta Q_p \tag{10}$$

This is the main reason why the specific enthalpy is the thermodynamic potential commonly used in geothermal reservoir engineering. The product specific enthalpy times water density ($H_w = h_w\, \rho_w$) is defined as volumetric enthalpy. If the fluid is contained in a porous/fractured rock, the actual fluid enthalpy in the reservoir is affected by porosity φ. Therefore, the water enthalpy density of the system at constant pressure or at any isobaric curve is equal to the product:

$$\varphi\, H_w(T) = \varphi\, \rho_w(T)\, h_w(T) \quad \left[\frac{k\,\mathrm{J}}{m^3}\right] \tag{11}$$

Equation (11) represents the heat stored in the fluid per cubic meter of porous rock as function of supercritical temperature. Figure 13 shows the curves of $\varphi\, H_w(T)$ for different supercritical pressures in a reservoir with 5% porosity. On the other hand, the heat stored in the solid skeleton per unit volume of porous rock is:

$$(1-\varphi)\; H_R(T) = (1-\varphi)\, c_R(T)\, \rho_R\, T \quad \left[\frac{k\,\mathrm{J}}{m^3}\right] \tag{12}$$

Where ρ_R is rock density and $c_R(T)$ is the isobaric rock specific heat capacity, which is also a function of temperature. A linear, practical correlation to compute $c_R(T)$ is given by this formula [6]:

$$c_R(T) = 10^{-3}(976.6065 + 0.752854\ T) \quad \left[\frac{kJ}{kg\ °C}\right] \tag{13}$$

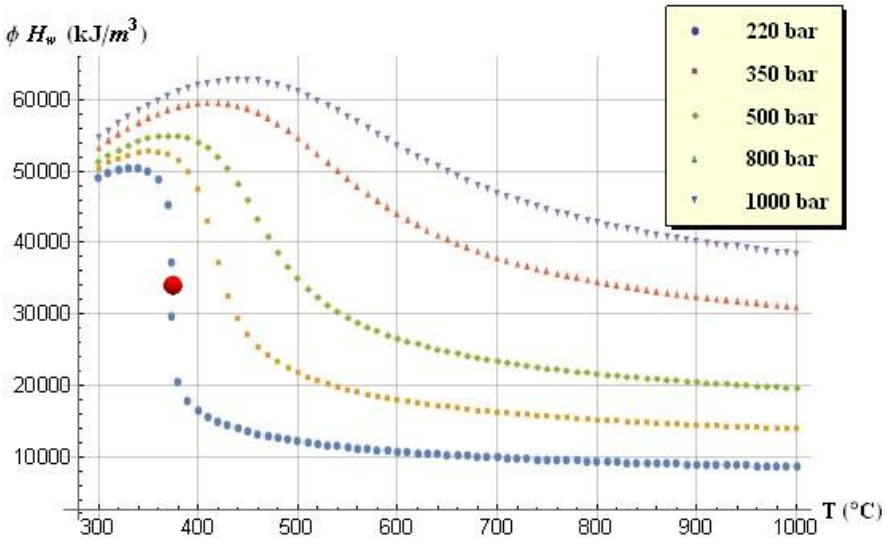

Figure 13. Supercritical volumetric fluid enthalpy in a reservoir with 5% porosity.

Assuming that correlation (13) is valid in a supercritical reservoir, the total volumetric heat stored in the fluid/rock system (figure 14) becomes a quadratic function of temperature:

$$Q_V(T) = \varphi\ H_w(T) + (1-\varphi)\ H_R(T) \quad \left[\frac{kJ}{m^3}\right] \tag{14}$$

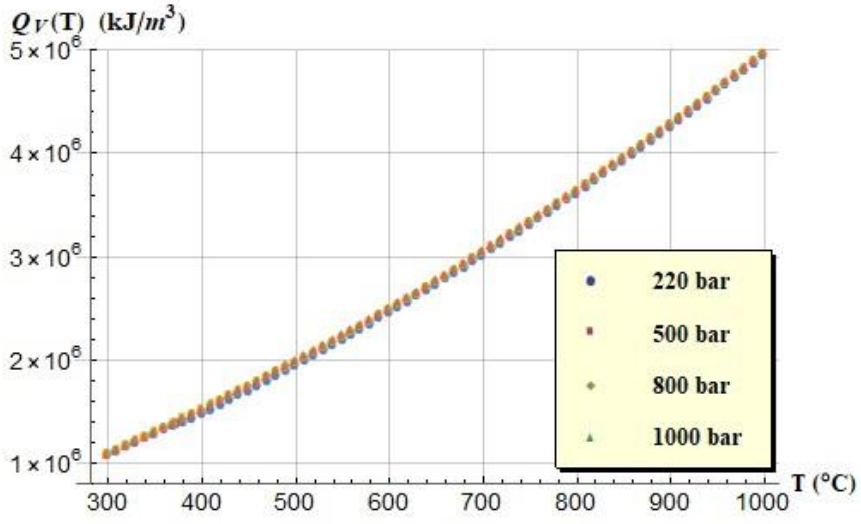

Figure 14. Total volumetric heat in a supercritical fluid/rock system with 5% porosity.

Figure 14 shows curves of $Q_V(T)$ for different supercritical pressures. It is observed that Q_V does not depend on pressure because the thermal energy is for the most part stored in the rock. Using the numerical outcomes of figures 13 and 14 we deduce that the fluid enthalpy density represents between 0.08% and 5% of the total stored heat.

4.1. Exergy of supercritical water

Exergy is the "*maximum work* (or power) output that could theoretically be obtained from a system at specified thermodynamic conditions relative to its surroundings. A system may receive (or discharge) fluids from (or to) the surroundings, and exchange heat and work with the surroundings." [7]. The state of the surroundings is the "dead state" because when a fluid is in equilibrium with the surroundings it may be considered dead, and the exergy from the system is zero. The specific exergy $E_x(T)$ and the maximum power output $dW_{Max}(T)/dt$ from a supercritical reservoir can be computed for a steady, open process as follows [7]:

$$E_x(T) = h_1 - h_0 - T_0(s_1 - s_0) \quad \left[\frac{\text{kJ}}{\text{kg}}\right] \quad \Rightarrow \quad \frac{dW_{Max}}{dt}(T) = \frac{dm}{dt} E_x(T) \quad [\text{kW}] \tag{15}$$

Where h_1 and s_1 are the specific enthalpy and entropy at the reservoir's outlet, h_0 and s_0 are the specific enthalpy and entropy of the surroundings considered as the dead state, T_0 is the temperature of the dead state and dm/dt is the reservoir mass flow rate. Exergy is also defined as *the maximum available useful work possible during a thermodynamic process that brings the system into equilibrium with a heat reservoir.* A heat reservoir is a system which its heat capacity is so large that when it is in thermal contact with other system its temperature remains constant. In this context, the atmosphere or the deep ocean can be considered as huge heat reservoirs. Both systems can be defined in a stable manner and approximated as unchangeable reference states or dead states.

We assume a submarine reservoir discharging directly its supercritical fluid into its surrounding, without considering any losses by friction inside wells or pipes. Figure 15 shows the behavior of the specific exergy from this reservoir as function of temperature, for different supercritical pressures. The thermal values of the dead state correspond to seawater at T_0 = 4°C, h_0 = 34.4 kJ/kg, s_0 = 0.046 kJ/kg/K, and a surrounding pressure of 220 bar [4]:

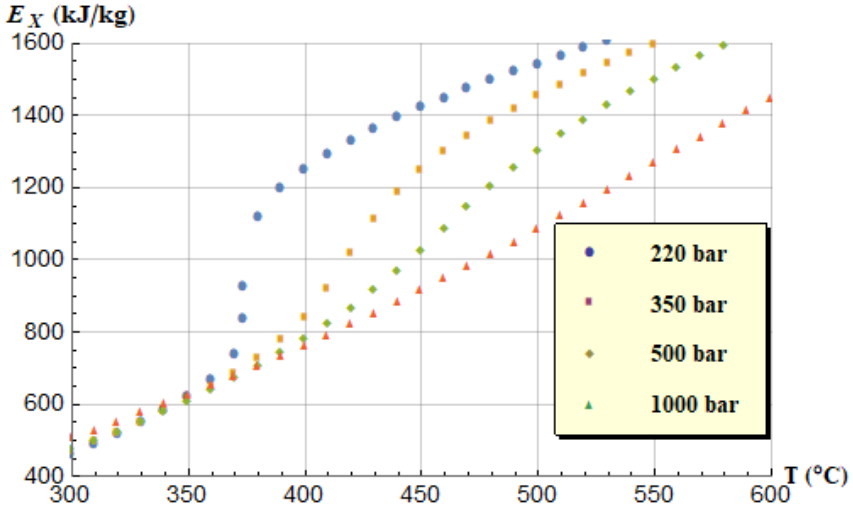

Figure 15. Power output (specific exergy) from a supercritical reservoir.

5. Conclusions

- Deep geothermal heat represents an immense energy potential. The fluids contained in profound reservoirs are at supercritical thermodynamic conditions. Volumetric enthalpy of supercritical water is larger than common geothermal fluid because of its higher density.

- Dry steam at 370°C and 40 bar has a density of 14.43 kg/m^3 and contains 45,354 kJ/m^3 of heat. The density of supercritical water at 350 bar and 400°C is 475 kg/m^3 and contains almost 10^6 kJ/m^3 of geothermal heat.
- Supercritical reservoirs at high temperature and pressure, beyond the critical point, could provide more than 20 times as much enthalpy per cubic meter as the geothermal fluids used with present current technology.
- Deep geothermal heat will be able to generate, in the next future, more electricity, more efficiently, cleaner energy, through special advanced turbine-generators adapted for supercritical fluids.

References

[1] IAPWS R6-95 2016 *Formulation 1995 for the Thermodynamic Properties of Ordinary Water Substance for General and Scientific Use* (The Netherlands 2009; Revised Release Dresden, Germany 2016: International Association for the Properties of Water and Steam) pp 1-18

[2] IAPWS-95 2011 *Release on the IAPWS Formulation 2011 for the Thermal Conductivity of Ordinary Water Substance* (Plzeň, Czech Republic: International Association for the Properties of Water and Steam) pp 1-15

[3] Suárez-Arriaga M C, Propiedades termodinámicas del agua geotérmica con la formulación IAPWS-95 programada y ampliada. *GEOTERMIA-Rev. Mex. de Geoenergía* **30/2**, 6-19

[4] Suárez-Arriaga M C, Bundschuh J and Samaniego F 2014. Assessment of submarine geothermal resources and development of tools to quantify their energy potentials for environmentally sustainable development. *J. of Cleaner Production* **83**, 21-32

[5] Harvey A H, Peskin A P and Klein S A 2004. NIST/ASME Steam Properties: Users' Guide, version 2.21, *NIST Standard Reference Database* **10**, National Institute of Standards and Technology, U.S. Department of Commerce

[6] Bundschuh J and Suárez-Arriaga M C 2010. *Introduction to the Numerical Modeling of Groundwater and Geothermal Systems – Fundamentals of mass, energy and solute transport in poroelastic rocks*. (London UK, Leiden, The Netherlands; 1st Edition, Multiphysics Modeling Series **2**, CRC Press/Balkema – Taylor & Francis Group) 1-479

[7] DiPippo R 2008. *Geothermal Power Plants - Principles, Applications, Case-Studies and Environmental Impact*, Chapter 10: *Exergy Analysis Applied to Geothermal Power Systems*. (Butterworth-Heinemann)